Magnetic properties of amorphous Ti_xSi_{100-x} and V_xSi_{100-x} alloys

2000 J. Phys.: Condens. Matter 12 4837

(http://iopscience.iop.org/0953-8984/12/22/316)

J. Phys.: Condens. Matter **12** (2000) 4837–4849. Printed in the UK PII: S0953-8984(00)10987-7

Magnetic properties of amorphous Ti_xSi_{100-x} and V_xSi_{100-x} alloys

A Yu Rogatchev and U Mizutani
Department of Crystalline Materials Science, Nagoya University, Nagoya 464-8603, Japan

Received 13 January 2000

Abstract. Magnetic properties have been measured in magnetic fields up to 70 kOe over the temperature range 1.8–300 K for a series of amorphous Ti_xSi_{100-x} ($3 \leqslant x \leqslant 41$) alloys and two amorphous V_xSi_{100-x} ($x = 7$ and $x = 12$) alloys. We found that the magnetic properties of amorphous Ti_xSi_{100-x} alloys change gradually as the Ti concentration varies across the metal–insulator transition ($x = 9.5$). The alloys are non-magnetic at high Ti content ($x > 25$), whereas the insulating alloys and even metallic ones near the metal–insulator transition exhibit a divergent magnetic susceptibility consistent with the formation of localized magnetic moments. At temperatures below 50 K, the susceptibility of these magnetic alloys follows the Curie–Weiss law well, with very small values of the Curie temperature. The fitting of the low-temperature magnetization data for the amorphous Ti_xSi_{100-x} and V_xSi_{100-x} alloys revealed that the magnetic moments are characterized by the spin value of 1/2 and a g-factor equal to 2. The room temperature electron spin-resonance measurements identified these moments as arising from the dangling bonds inherent to the network of amorphous Si and ruled out the possibility of the alloys having the d-state magnetism associated with Ti and/or V atoms.

1. Introduction

Amorphous metal–Si or metal–Ge alloys and doped crystalline semiconductors constitute two complementary groups of disordered materials and equally exhibit the continuous metal–insulator transition (MIT), when the concentration of a metal element or dopant exceeds some critical value n_c. In the former, the MIT takes place at a metal content of 10–20 at.%, which corresponds to a critical electron concentration $n_c = 10^{21}$–10^{22} cm^{-3}, which is almost three orders of magnitude higher than that in doped semiconductors. In spite of the large difference in n_c, various properties such as the resistivity [1–3], the single-particle density of states [4,5], and the specific heat [6–9] behave in a similar fashion for both groups of materials. Recent experiments have indicated that the localized magnetic moments strongly affect the low-temperature transport in the doped semiconductors [10,11] as well as in amorphous alloys [12]. Hence, one may expect a great similarity in magnetic properties of those materials.

The magnetic properties of the doped crystalline semiconductors—in particular, those of Si:P—have been intensively studied in the past by means of ESR [13, 14], NMR [15, 16], and specific heat [7, 17] and magnetic measurements [18, 19]. In the insulating regime well below the MIT, the magnetic properties of Si:P are known to originate from electronic states localized around individual impurity P atoms. When the system goes towards the MIT from the insulating side, the ratio of the number of localized magnetic moments to the total number of P atoms strongly decreases, but it remains finite even on the metallic side of the MIT. It was shown that the magnetic susceptibility χ no longer follows the Curie–Weiss law, and

0953-8984/00/224837+13$30.00

it is often approximated by the expression $\chi \propto T^{-\alpha}$ with $0 < \alpha < 1$ below 4 K [18, 19]. The sub-Curie-temperature dependence was interpreted within the Bhatt–Lee model [20] by assuming a random antiferromagnetic spin-pair coupling.

Less is known about the magnetic properties of the amorphous alloys. Like in doped crystalline semiconductors, the magnetic susceptibility of amorphous V_xSi_{100-x} [9] and Nb_xSi_{100-x} [21] alloys shows a divergent temperature dependence in both insulating and weakly metallic samples. In addition, Allen *et al* [21] revealed that their susceptibility data on amorphous Nb_xSi_{100-x} alloys follow the Bhatt–Lee model well, below about 50 K, and claimed its universality for different insulating disordered systems. However, the magnetic susceptibility data on amorphous V_xSi_{100-x} alloys were found to obey the Curie–Weiss law [9].

In this paper, we present the results of magnetic and ESR measurements on a series of amorphous Ti_xSi_{100-x} and V_xSi_{100-x} alloys across the MIT. The same series of samples were recently employed in resistivity and specific heat measurements [22], on the basis of which the MIT in amorphous Ti_xSi_{100-x} alloys was claimed to occur at $x = 9.5$. The aim of this work is to test whether the Bhatt–Lee model is applicable to amorphous Ti_xSi_{100-x} and V_xSi_{100-x} alloys and to clarify the origin of the localized moments in these amorphous alloys.

2. Experimental procedure

Amorphous Ti_xSi_{100-x} ($x = 3$, 6, 9.5, 13.3, 17.5, 27.5, 32, and 41) samples were grown by triode DC sputtering from composition targets prepared by arc melting of an appropriate amount of 99.999% Si and 99.9% Ti. The deposition was performed at the rate of 15–20 Å s^{-1} on a copper substrate at room temperature. The thickness of the sample was in the range 200–300 μm. The composition was determined by energy-dispersive analysis of x-rays (EDAX) and ion-coupled plasma (ICP) analysis with an accuracy of about 0.5 atomic per cent. The amorphous structure of the sputtered sample was confirmed by x-ray diffraction and electron microscopy. The samples were mechanically removed from the substrate, crushed, and compacted into a plastic holder with a negligible magnetic moment. Magnetic measurements were performed using a SQUID magnetometer (QUANTUM DESIGN MPMS-7) on each of the samples, with weights of 200–300 mg. The magnetization was measured in the temperature range 1.8–300 K and in a magnetic field up to 70 kOe. The ESR measurements were performed at room temperature using a Bruker E500 X-band spectrometer.

3. Results and discussion

3.1. Separation of the ferromagnetic contribution from the total magnetization

The field dependence of the magnetization M at $T = 300$ K is presented in figure 1 for several amorphous Ti_xSi_{100-x} alloys. It can be seen from figure 1 that a small ferromagnetic contribution exists at low fields below 5–7 kOe. Hence, we may reasonably decompose M into two terms:

$$M = M_{ferro} + \chi H \tag{1}$$

where the first term M_{ferro} represents the ferromagnetic contribution and the second the paramagnetic one proportional to the applied field H. The ferromagnetic contribution M_{ferro} apparently saturates with increasing applied field and the total magnetization shows an expected linear variation above about 10 kOe. The ferromagnetic term is found to exist also for the amorphous V_xSi_{100-x} alloys. Allen *et al* [21] also reported the existence of the ferromagnetic term in the field dependence of the magnetization at 300 K for amorphous Nb_xSi_{100-x} alloys prepared by sputtering.

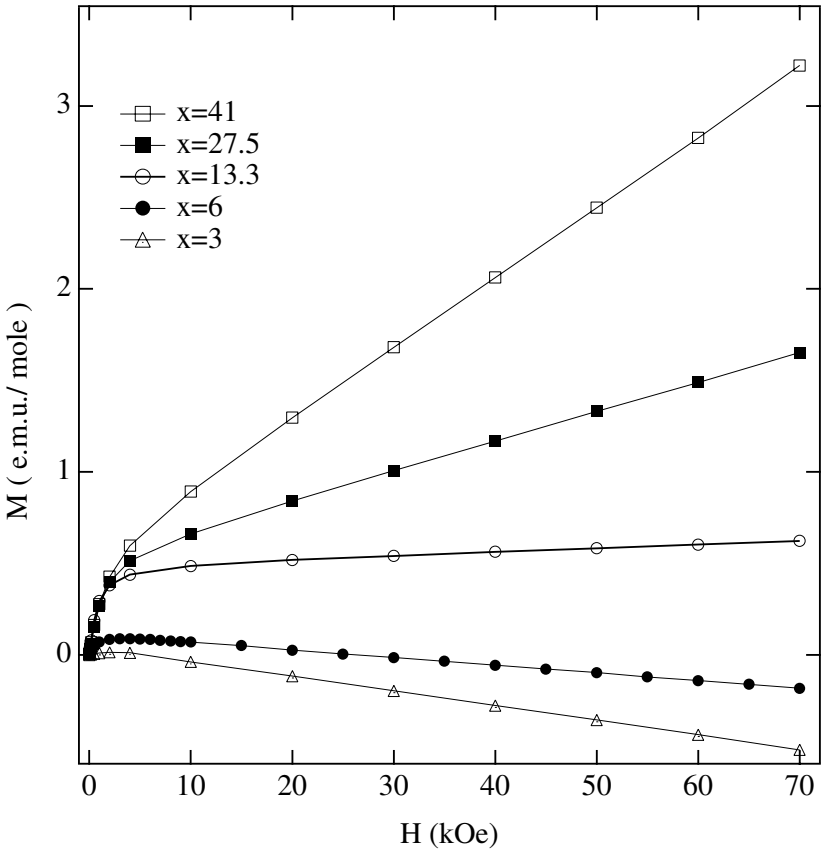

Figure 1. The magnetic field dependence of the magnetization for selected amorphous Ti_xSi_{100-x} alloys at $T = 300$ K. The curves are drawn through the experimental points to guide the eye.

To shed some light on the ferromagnetic term, we have studied the magnetic properties of the C49 and C54 $TiSi_2$ compounds, both of which can be obtained by crystallizing the amorphous $Ti_{32}Si_{68}$ alloy. Upon heating, it transformed into the C49 $TiSi_2$ metastable phase at about 600 K and, subsequently, into the C54 $TiSi_2$ compound at about 1000 K. Figure 2 shows the field dependence of the magnetization for both compounds thus prepared, together with the data for the amorphous $Ti_{32}Si_{68}$ alloy. In addition, the data for the stable C54 $TiSi_2$ compound prepared by arc melting are incorporated. One can see that the ferromagnetic term exists for all three phases, but it is absent in the C54 compound prepared by arc melting. Thus, we can definitely say that the ferromagnetic contribution is extrinsic in nature and arises only when samples are prepared by sputtering. If we assume that the ferromagnetic term M_{ferro} is due entirely to the bcc Fe inclusions introduced during sputtering, we can roughly estimate the Fe concentration to be at most 0.0003–0.005 at.% or 3–50 ppm from the magnitude of M_{ferro}. Unfortunately, however, the ICP analysis failed to detect such a small amount of ferromagnetic impurity within the accuracy of the measurements. It may also be worth mentioning that this term has nothing to do with a possible formation of magnetic oxides on the surface of the sample, since the intentional heat treatment of the finely crushed $x = 27$ sample at 500 K in air did not change the absolute value of M_{ferro}. Further work is under way in pursuing the origin of the ferromagnetic contribution.

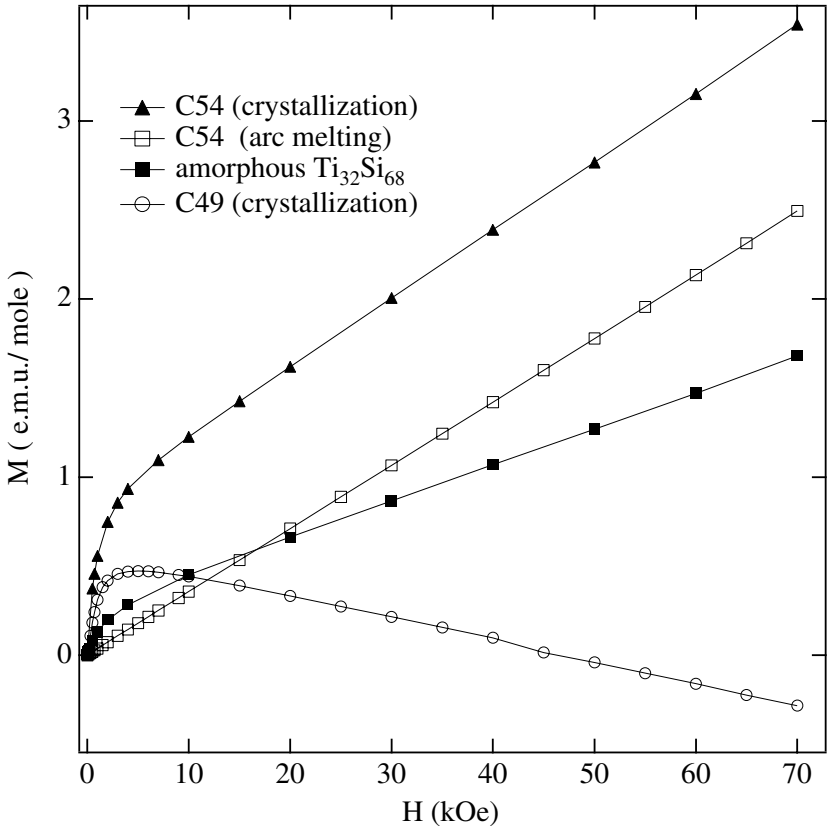

Figure 2. The magnetic field dependence of the magnetization at $T = 300$ K for a-$Ti_{32}Si_{68}$ alloy and C49 $TiSi_2$ and C54 $TiSi_2$ intermetallic compounds prepared by crystallizing a-$Ti_{32}Si_{68}$ and by arc melting. The curves are drawn through the experimental points to guide the eye.

Regardless of whether the ferromagnetic term is present or not, the high-field variations of the two C54 samples prepared by sputtering and arc melting are indeed in parallel with each other, indicating possession of the same magnetic susceptibility χ for these two samples. This encourages us to extract the intrinsic magnetic properties of both amorphous alloys and crystalline compounds in the Ti–Si and V–Si systems simply by subtracting the temperature-independent ferromagnetic contribution below 300 K.

The magnetic susceptibility χ at 300 K for amorphous Ti_xSi_{100-x} alloys is deduced by using a line fit to the magnetization data above 10 kOe in figure 1. The results are shown in figure 3 as a function of the Ti content. The data for the two $TiSi_2$ compounds and for crystalline Si are also included. The magnetic susceptibility is given by the sum of two contributions:

$$\chi = \chi_{core} + \chi_{el} \tag{2}$$

where χ_{core} is due to the Larmor diamagnetism of core electrons, and χ_{el} represents the electronic contribution arising from the Pauli spin paramagnetism, the Landau diamagnetism, and the orbital paramagnetism of the conduction electrons. The orbital (paramagnetic) term may appear only for materials with partially filled non-s bands [23]. This contribution is indeed large in non-ferromagnetic transition metals, sometimes larger than the spin susceptibility [24].

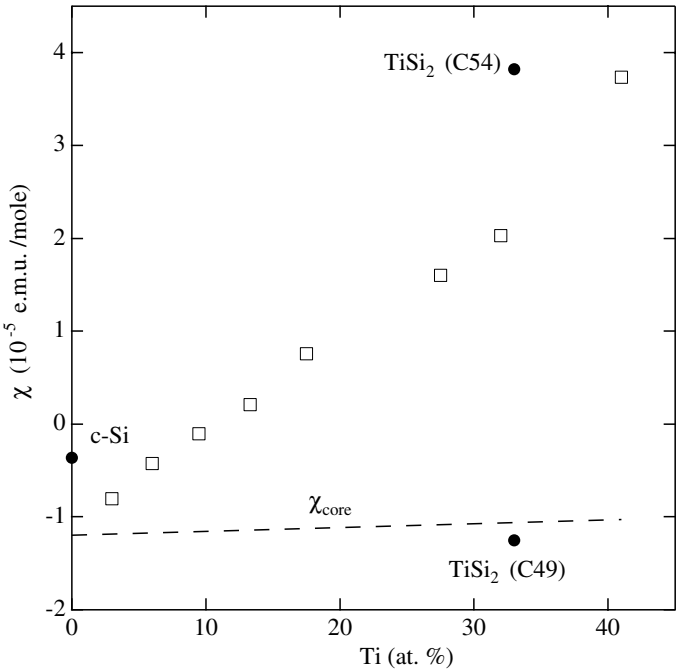

Figure 3. The Ti concentration dependence of the magnetic susceptibility at $T = 300$ K for amorphous Ti_xSi_{100-x} alloys. The magnetic susceptibilities of the C49 and C54 $TiSi_2$ intermetallic compound and crystalline Si are also shown. The dashed line shows the estimated Larmor diamagnetic contribution.

The values of χ_{core} for the two crystalline compounds should be the same and, hence, the observed much lower total magnetic susceptibility of the C49 $TiSi_2$ compound can be ascribed to the possession of a smaller density of electronic states at the Fermi level. It is interesting to note in this context that the magnetic susceptibility of the amorphous $Ti_{32}Si_{68}$ alloy is close to an average of the values for the two crystalline compounds. Surprisingly, the value of χ for the insulating samples with $x \leqslant 6$ is smaller than the value for the crystalline Si. The measurement of the room temperature magnetic susceptibilities χ_c and χ_a of the crystalline and the amorphous forms of Ge, respectively, revealed the ratio $\chi_a/\chi_c = 2.7 \pm 0.3$ [25]. The enhanced diamagnetism was discussed in relation to the details of the bonding in the bulk amorphous Ge [26]. By extrapolating our data to zero Ti concentration, we were able to obtain $\chi_a = -1.2 \times 10^{-5}$ emu mol^{-1} for amorphous Si and, in turn, the ratio $\chi_a/\chi_c \approx 3$. This happens to be fairly close to the ratio reported for Ge.

The Larmor diamagnetic susceptibility χ_{core} for a series of amorphous Ti_xSi_{100-x} alloys can be estimated by taking a weighted mean of contributions of the two constituent elements. Here we assume $\chi_a = 0.7 \times 10^{-5}$ emu mol^{-1} for Ti (Ti^{4+} [27]) and $\chi_{Si} = \chi_a$ for Si. The calculated χ_{core} is shown in figure 3 as a dashed line. We see that χ_{core} is essentially independent of the Ti concentration in the amorphous Ti–Si system. The strong decrease of $\chi - \chi_{core}$ with decreasing Ti concentration obviously reflects the variation of χ_{el}. Therefore, we are led to conclude that the density of the electronic states at the Fermi level decreases smoothly without any discontinuity across the MIT at about $x = 9$ in the amorphous Ti_xSi_{100-x} alloys, and remains finite in the insulating regime. This agrees well with the variation of the electronic specific heat coefficient γ found in the specific heat measurements [22].

3.2. The temperature dependence of the magnetic susceptibility below 300 K

Figure 4 shows the magnetic susceptibility χ measured at $H = 2$ kOe for a series of amorphous Ti_xSi_{100-x} alloys as a function of the logarithm of the temperature in the temperature range 1.8–300 K. The data are presented after the subtraction of the ferromagnetic contribution at room temperature. The magnetic susceptibilities of both C54 and C49 $TiSi_2$ compounds were also measured and found to be temperature independent. This is consistent with the non-magnetic behaviour of the amorphous alloys with high Ti concentrations. However, a strong divergent temperature dependence appears at low temperatures with decreasing Ti concentration, particularly upon entering the insulating regime, suggesting the presence of local magnetic moments. As is clear from figure 4, this temperature dependence is already present in samples with $x = 9.5$ and 13.3, both of which are located on the metallic side of the MIT.

We have analysed the temperature dependence of the observed magnetic susceptibility for the two insulating ($x = 3, 6$) and the two metallic ($x = 9.5, 13.3$) samples in terms of the

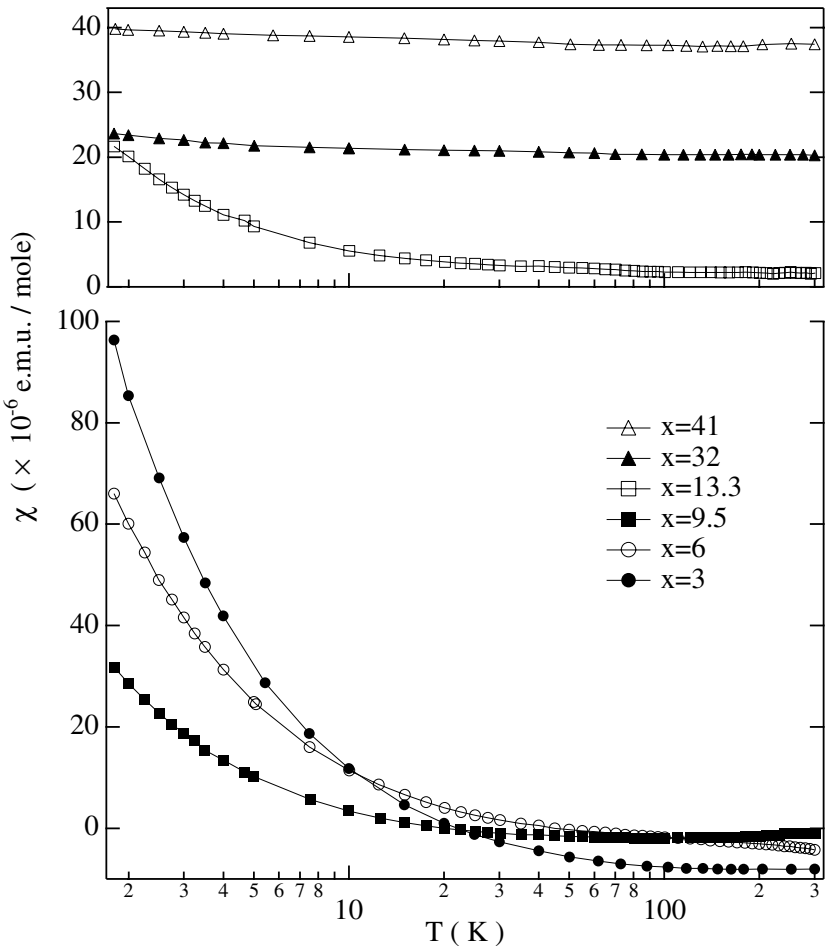

Figure 4. The temperature dependence of the magnetic susceptibility for selected amorphous Ti_xSi_{100-x} alloys. The curves are drawn through the experimental points to guide the eye.

following two equations. First, we employ the usual Curie–Weiss law:

$$\chi = \chi_0 + C/(T - \Theta) \tag{3}$$

where C is the Curie constant and Θ is the Curie temperature. Equation (3) implies that the interaction between the local moments is characterized by a single value of the exchange coupling. Alternatively, the Bhatt–Lee model can be tested. The magnetic susceptibility is then given by

$$\chi = \chi_0 + C/T^{\alpha} \tag{4}$$

where the sub-Curie-temperature dependence arises from a broad distribution of the exchange coupling and $0 < \alpha < 1$ for antiferromagnetic interactions. To avoid uncertainty in the choice of χ_0, the fitting was performed in the temperature range $1.8 < T < 50$ K by using χ_0, α, Θ, and C as free parameters.

We revealed that the Curie–Weiss law always works better, as judged from the derivation of consistently lower values of the standard deviation. The susceptibility data are plotted in figure 5 in the form of $1/(\chi - \chi_0)$ against temperature in the range $0 \leqslant T \leqslant 10$ K, by using the value of χ_0 obtained from the fitting. It can be seen that the data clearly obey the Curie–Weiss law with a small ($|\Theta| < 1$ K) negative Curie temperature. Indeed, equations (3) and (4) yield parameters very close to the free magnetic moments with $\alpha \approx 1$ and $\Theta \approx 0$ for the two metallic

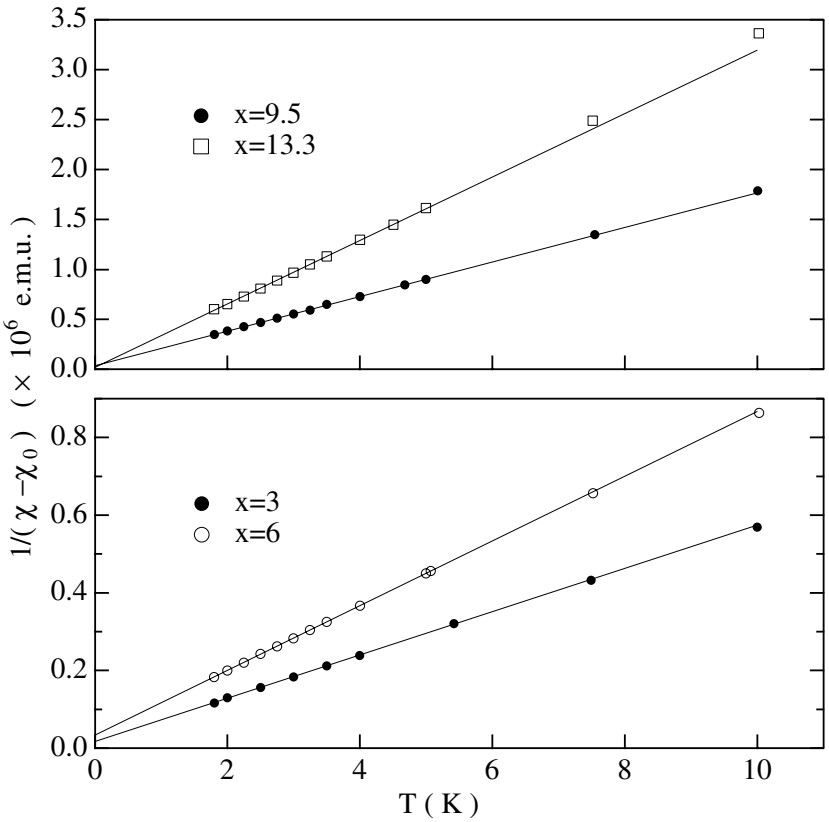

Figure 5. The temperature dependence of $1/(\chi - \chi_0)$ for amorphous Ti_xSi_{100-x} alloys in the temperature range below 10 K. The solid lines are the least-squares fits to equation (3).

samples. We also confirmed that a good fit to the Curie law can be equally obtained, if the temperature range is extended to 50 K. The numerical results are summarized in table 1. The magnetic susceptibility of the two amorphous V_xSi_{100-x} alloys with $x = 7$ and $x = 12$, both on the insulating side of the MIT, behaved in the same manner as above.

Table 1. Magnetic data for a-Ti_xSi_{100-x} alloys extracted from the fitting of the magnetic susceptibility in the range $1.8 < T < 50$ K. C: the Curie constant; Θ: the Curie temperature.

x	C (10^{-5} emu mol^{-1})	Θ (K)
3	22	-0.3 ± 0.1
6	15	-0.4 ± 0.1
9.5	6.6	-0.15 ± 0.1
13.3	3.7	-0.1 ± 0.1

Our results on amorphous Ti_xSi_{100-x} and V_xSi_{100-x} alloys are apparently at variance with the results on amorphous Nb_xSi_{100-x} alloys reported by Allen *et al* [21]. They stressed that the Bhatt–Lee model describes the susceptibility of amorphous Nb_xSi_{100-x} alloys ($1.7 \leqslant T \leqslant 50$ K) better than the Curie–Weiss law and found the exponent α in the range from 0.85 for the insulating Nb_5Si_{95} alloy to 0.51 for the metallic $Nb_{20}Si_{80}$ alloy. The discrepancy between the Ti–Si and Nb–Si systems is not caused by the choice of χ_0, because χ_0 is chosen as a free fitting parameter and, in the present case, α and Θ depend only slightly on χ_0. Despite the disagreement as regards the temperature dependence, the Curie constant C was almost the same at a chosen content of metal atoms for all three relevant systems. Allen *et al* [21] pointed out that the local magnetic moments may originate from small clusters of Nb atoms in amorphous Nb_xSi_{100-x} alloys. To verify whether the local atomic structure modifies the magnetic susceptibility behaviour, we measured the susceptibility of the amorphous alloy with $x = 9.5$ after the heat treatment at 700 K below its crystallization temperature of 900 K. Although the Curie constant is slightly reduced after the heat treatment, the Curie–Weiss law was found to remain valid.

3.3. Magnetization behaviour at low temperatures

As one can see from table 1, the fitting of the temperature dependence of χ yields very small values of the Curie temperature ($|\Theta| < 1$ K) and, hence, it is important to examine more precisely how the magnetic interaction among the moments changes in the lowest-temperature range. For this purpose, $M(H, T)$ was measured for four amorphous Ti_xSi_{100-x} samples as a function of H in the region of 0.2 and 70 kOe at $T = 1.8$, 3.6, 5.4, and 7.6 K. Similar measurements were also performed for the amorphous V_xSi_{100-x} samples at $T = 1.8$, 4.15, and 5.4 K. The local magnetic moment contribution M_s was deduced by subtracting from the measured value the ferromagnetic contribution and the second term in equation (1), where χ represents the temperature-independent magnetic susceptibility given by equation (2).

Figure 6 shows the resulting M_s-data measured at different temperatures as a function of H/T. This plot allows us to analyse the data without making any arbitrary assumption about the values of the total angular momentum J and the g-factor. One can see from figure 6 that the data for amorphous Ti_xSi_{100-x} and V_xSi_{100-x} alloys show qualitatively similar behaviours, regardless of whether they are in a metallic or insulating regime. Above 3–4 K, the magnetization curves fall on a single common line. This is taken as evidence that the magnetic moment behaves as a free moment in this temperature range. However, the M_s-curve goes slightly below the common line at 1.8 K, indicating the appearance of the antiferromagnetic coupling in the alloys.

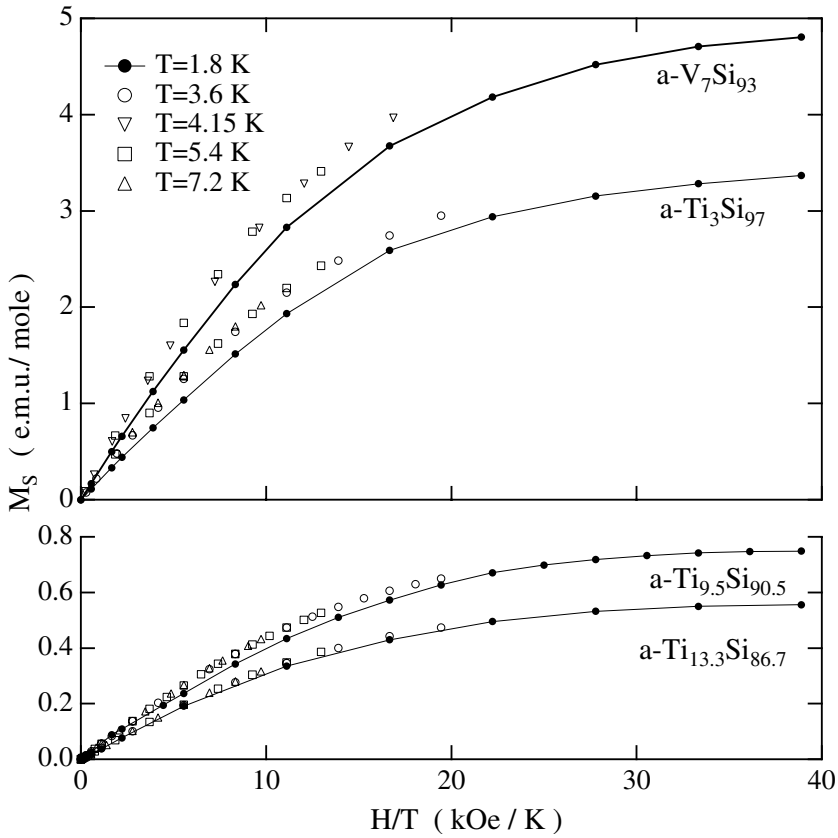

Figure 6. The local moment magnetization $M_s(H)$ as a function of H/T for a-Ti_xSi_{100-x} and a-V_xSi_{100-x} alloys at several indicated temperatures. For each sample at $T > 3$–4 K the data fall on a single curve. The data at $T = 1.8$ K go below the common curve signalling the appearance of the antiferromagnetic coupling. The solid lines are drawn through the data at $T = 1.8$ K to guide the eye.

The revealed energy scale of the magnetic interaction explains the behaviour of the specific heat in insulating amorphous V_xSi_{100-x} [9] and Ti_xSi_{100-x} [22] alloys. The specific heat, when plotted in the form of C/T versus T^2, shows an ordinary linear variation due to electronic and lattice terms in the temperature range above 2.5 K for these alloys. Indeed, in this temperature range, free magnetic moments produce no contribution to the specific heat in zero magnetic field. Below 2.5 K, however, the specific heat data show an upturn, which can most probably be attributed to the appearance of the antiferromagnetic interaction in the system.

3.4. The origin of the magnetic moment

The next question that we address is that of what entity is responsible for the local magnetic moment in the amorphous Ti_xSi_{100-x} and V_xSi_{100-x} alloys. To characterize the magnetic states, the $M_s(H)$ data at $T = 3.6$ and 4.15 K, where the magnetic interactions are negligible, were fitted to the equation

$$M_s(H) = \mu_B g J N_s B_J(\mu_B g J H/k_B T) \tag{5}$$

where N_s is the concentration of the magnetic moments and $B_J(y)$ is the Brillouin function. We have considered different combinations of the total angular momentum J and the g-factor, including the free spin, and the ground state of the free Ti atom ($J = 2$, $g = 2/3$) and the free V atom ($J = 3/2$, $g = 0.4$). In addition, we have employed data relating to ten impurity states of substitutional and interstitial Ti and V atoms in different charge and spin states in the matrix of crystalline Si [28,29]. N_s was chosen as a free parameter in the fitting. Surprisingly, we found that, among the combinations considered, the Brillouin function with the parameters of the free spin, i.e., $J = s = 1/2$ and $g = 2$, produces the best fit for both metallic and insulating alloys in the amorphous Ti_xSi_{100-x} and V_xSi_{100-x} systems. The results of the fitting are shown in figure 7 and the numerical values are summarized in table 2. The concentration of the metal atoms in the alloys, N_{Me}, is also included for comparison. The concentrations of the localized magnetic moments in the amorphous Ti_xSi_{100-x} and V_xSi_{100-x} alloys turned out to be unexpectedly small. One can see from table 2 that the ratio N_s/N_{Me} is only about 1% even at metal concentrations well below the MIT.

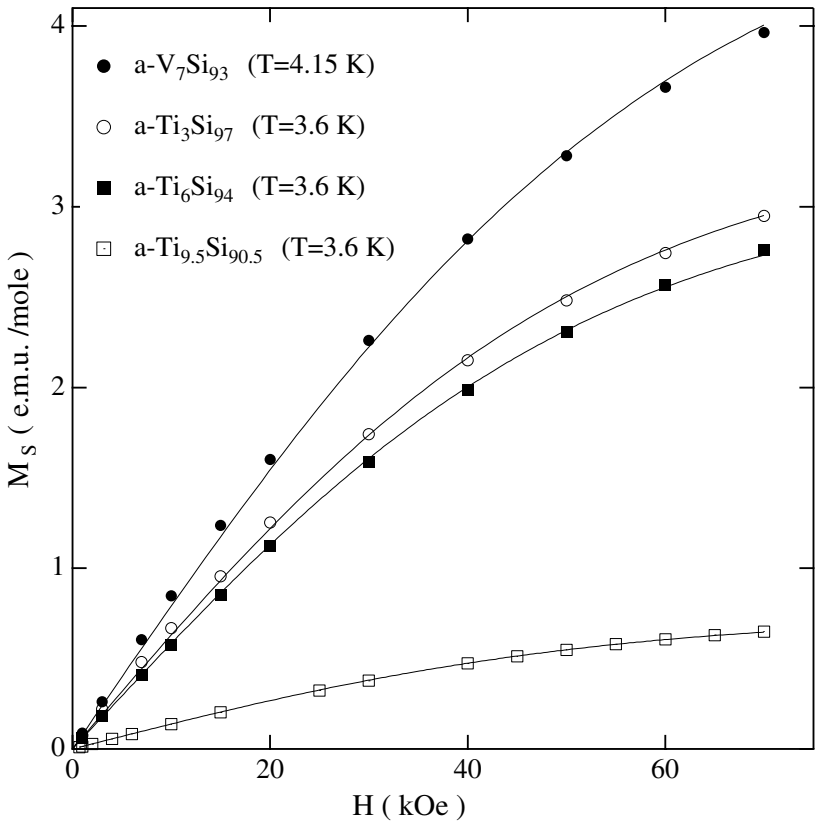

Figure 7. The least-squares fit of $M_s(H)$ to equation (5) (solid lines) with the spin value of 1/2 and g-factor of 2 for the amorphous alloys indicated, at temperatures where the magnetic interactions are negligible.

We further proceed to verify whether the revealed free-spin parameters are consistent with the magnetization data at lower temperatures, where the magnetic coupling becomes substantial. We plotted in figure 8 the $M_s(H)$ values measured at $T = 1.8$ K for three samples. The theoretical Brillouin function with $s = 1/2$ and $g = 2$, and the concentration

Table 2. The spin concentration N_s in a-Ti_xSi_{100-x} and a-Ti_xSi_{100-x} alloys as extracted from the fitting of the low-T magnetization. N_{Me} is the concentration of Ti or V atoms.

x	N_s (10^{19} cm^{-3})	N_{Me}(10^{21} cm^{-3})
a-Ti_xSi_{100-x}		
3	2.9	1.46
6	2.6	2.84
9.5	0.66	4.7
13.3	0.54	6.8
a-V_xSi_{100-x}		
7	4	3.2
12	2.8	6.1

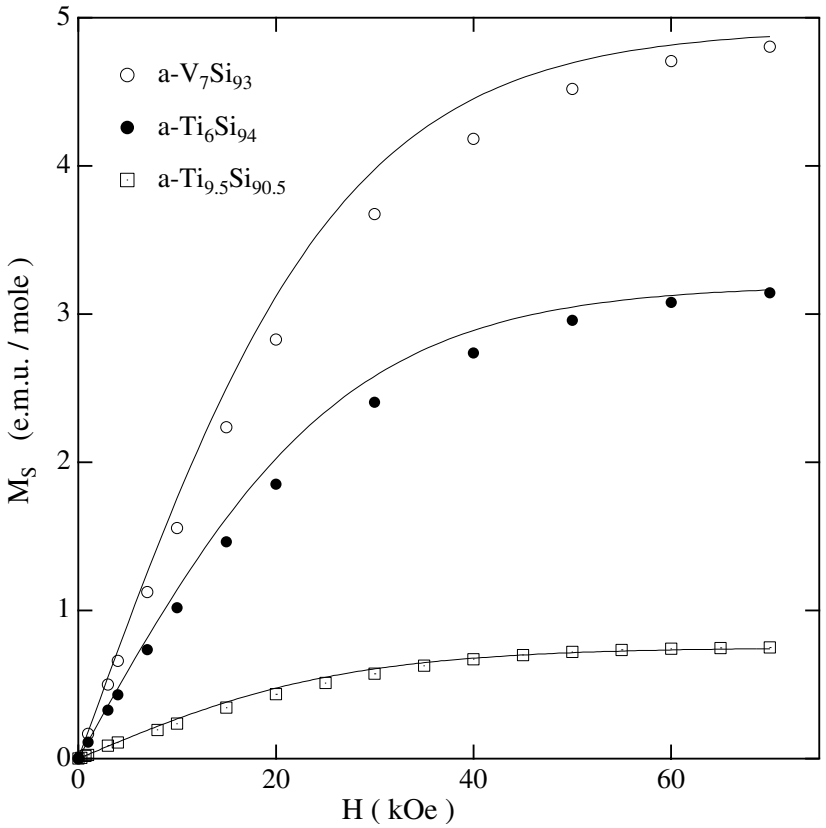

Figure 8. The $M_s(H)$ data at $T = 1.8$ K for the amorphous alloys indicated. The solid lines are the Brillouin function with $s = 1/2$, $g = 2$ and the concentration of the magnetic moments as extracted from the fitting at $T \geqslant 3.6$ K.

of spins extracted from the fitting in the paramagnetic range are superimposed. One can see from figure 8 that the experimental data clearly deviate from the Brillouin function at low and intermediate magnetic fields. However, $M_s(H)$ saturates and reaches the theoretical paramagnetic limit at high fields of 60–70 kOe. Since the thermal energy at 4 K is high enough to destroy completely the magnetic coupling in the alloys (see figure 6), a magnetic field of

the order of $4k_B/\mu_B \approx 60$ kOe should equally overcome magnetic interactions and, thereby, aligns the spins and produces a value of M_s close to the free-spin case.

Guided by the observations on doped crystalline semiconductors, one may naturally think that the observed magnetic moments in amorphous alloys originate from 3d electrons localized around metal atoms. The soft x-ray spectroscopy measurements [9] as well as the theoretical calculation on the basis of the crystalline-Si:V superlattice model [29] showed that, at $x = 7$, the average V–V distance is short enough to produce a d band with a width of about 2 eV. However, the on-site Coulomb energy is found to be only 0.2–0.3 eV for both Ti and V in crystalline Si [29]. Therefore, we believe that the on-site Coulomb energy is too small to lead to the formation of a local moment on either Ti or V atoms. In addition, the free-spin-like response and very low concentrations of spins observed for both amorphous Ti_xSi_{100-x} and V_xSi_{100-x} alloys are hardly reconcilable with the d-state magnetism associated with Ti and V atoms.

In order to identify magnetic moments involved in the present amorphous alloys, we have performed electron spin-resonance (ESR) measurements for the amorphous Ti_6Si_{94} and V_7Si_{93} alloys at 300 K. The ESR spectrum consists of a single resonance line. The resonance line is symmetric and isotropic. The corresponding values of the g-factor (2.005(5)) and linewidth (8.6 G) are in excellent agreement with the values for dangling bonds in sputtered amorphous Si reported by Brodsky and Title [30]. Similar parameters were also found for the amorphous V_7Si_{93} alloy.

The spin density N_s due to dangling bonds in amorphous Si is known to depend strongly on the preparation conditions. According to the ESR measurements, N_s ranges from less than 5×10^{17} cm^{-3} for samples of glow-discharge amorphous Si [26] to the value $N_s = 3 \times 10^{20}$ cm^{-3} for sputtered amorphous Si [30]. The value of N_s deduced from the susceptibility measurement for the present amorphous Ti_3Si_{97} is 2.9×10^{19} cm^{-3}, as listed in table 2, which is almost equal to the value 2.6×10^{19} cm^{-3} for sputtered amorphous Si measured by Hudgens [31]. We conclude from the ESR and the low-temperature magnetization data that the localized magnetic moments in amorphous Ti_xSi_{100-x} and V_xSi_{100-x} alloys stem from the dangling bonds of the amorphous Si network.

The identification of the magnetic moments as arising from the dangling bond of the amorphous Si is in accord with the structural studies performed earlier on a series of amorphous V_xSi_{100-x} alloys [9]. The structural studies revealed that the V atoms are substituted for Si atoms in the tetrahedrally bonded Si network in the range where $x < 10$, whereas the local atomic structure resembles that of the VSi_2 intermetallic compound in the range $20 < x < 40$. These two local atomic structures are apparently competing with each other in the range $10 < x < 20$. We expect similar structural modification in amorphous Ti_xSi_{100-x} alloys. Since the number of local units with the structure of amorphous Si progressively decreases with increasing metal content, the concentration of dangling bonds and, hence, the local moments should also decrease. This is indeed observed for both amorphous Ti_xSi_{100-x} and V_xSi_{100-x} alloys.

4. Summary and conclusions

We have measured the magnetic susceptibility in the temperature range 1.8–300 K and the magnetization up to 70 kOe for a series of amorphous Ti_xSi_{100-x} and V_xSi_{100-x} samples. At Ti concentrations $x \geqslant 25$, the alloys are non-magnetic, whereas the magnetic susceptibility follows the Curie–Weiss law well, below 50 K, for the insulating alloys and for the metallic ones slightly above the MIT. The magnetization data on both amorphous Ti_xSi_{100-x} and V_xSi_{100-x} samples demonstrated that the magnetic moments are characterized by a spin value of 1/2 and

a g-factor equal to 2. The ESR measurements showed that the localized magnetic moment originates from the dangling bonds of the amorphous Si network. We also pointed out that the Ti and V 3d states carry no magnetic moment in the present amorphous alloys.

Acknowledgments

The authors are grateful to S Kuroda and K Marumoto for ESR measurements. They are also grateful to S Kuroda and H Ikuta for useful discussion. AR thanks the C&C Foundation for financial support.

References

[1] Ionov A N, Matveev M N, Rentch R and Shlimak I S 1986 *Sov. Phys.–JETP* **42** 466
[2] Elefant D, Gladun C, Heinrich A, Schumann J and Vinzelberg H 1991 *Phil. Mag.* **64** 49
[3] Thomas G A, Paalanen M and Rosenbaum T F 1983 *Phys. Rev.* B **27** 3897
[4] Hertel G, Bishop D J, Spencer E G, Rowell J M and Dynes R C 1983 *Phys. Rev. Lett.* **50** 743
[5] Massey J G and Lee M 1995 *Phys. Rev. Lett.* **75** 4266
[6] Kobayashi N, Ikehata S, Kobayashi S and Sasaki W 1977 *Solid State Commun.* **24** 67
[7] Lakner M, von Löhneysen H, Langenfield A and Wölfle P 1994 *Phys. Rev.* B **50** 17 064
[8] Mael D, Yoshizumi S and Geballe T H 1986 *Phys. Rev.* B **34** 467
[9] Mizutani U, Ishizuka T and Fukunaga T 1997 *J. Phys.: Condens. Matter* **9** 5333
[10] Dai P, Zhang Y and Sarachik M P 1992 *Phys. Rev. Lett.* **69** 1804
[11] Lakner M and von Löhneysen H 1993 *Phys. Rev. Lett.* **22** 3475
[12] Yakimov A I, Wright T, Adkins C J and Dvurechenskii A V 1994 *Phys. Rev.* B **51** 16 549
[13] Quirt J P and Marko J R 1973 *Phys. Rev.* B **7** 3842
[14] Paalanen M A, Sachdev S, Bhatt R N and Ruckenstein A E 1986 *Phys. Rev. Lett.* **57** 2061
[15] Hirsch M J and Holcomb D F 1987 *Phys. Rev.* B **33** 2520
[16] Alloul H and Dellouve P 1987 *Phys. Rev. Lett.* **59** 578
[17] Kobayashi N, Ikehata S, Kobayashi S and Sasaki W 1979 *Solid State Commun.* **32** 1147
[18] Andres K, Bhatt R N, Goalwin P, Rice T M and Walstedt R E 1981 *Phys. Rev.* B **24** 244
[19] Sarachik M P, Roy A, Turner M, Levy M, He D, Isaacs L L and Bhatt R N 1986 *Phys. Rev.* B **34** 387
[20] Bhatt R N and Lee P A 1982 *Phys. Rev. Lett.* **48** 344
[21] Allen L C, Paalanen M A and Bhatt R N 1993 *Europhys. Lett.* **21** 927
[22] Rogatchev A Yu, Takeuchi T and Mizutani U 2000 *Phys. Rev.* B **61** 10 010
[23] Kubo R and Obata Y 1956 *J. Phys. Soc. Japan* **11** 547
[24] Shimizu M 1981 *Rep. Prog. Phys.* **44** 329
[25] Hudgens S J 1973 *Phys. Rev.* B **7** 2481
[26] Mott N F and Davis E A 1979 *Electronic Processes in Non-Crystalline Materials* (Oxford: Clarendon)
[27] Angus W R 1932 *Proc. R. Soc.* A **136** 569
[28] Ludwig G H and Woodbury H H 1962 *Solid State Physics* vol 13 (New York: Academic) p 223
[29] Zanger A 1986 *Solid State Physics* vol 39 (New York: Academic) p 276
[30] Brodsky M H and Title R S 1969 *Phys. Rev. Lett.* **23** 581
[31] Hudgens S J 1976 *Phys. Rev.* B **14** 1547